Macrophages in bone fracture healing: Their essential role in endochondral ossification

Claudia Schlundt, Thaqif El Khassawna, Alessandro Serra, Anke Dienelt, Sebastian Wendler, Hanna Schell, Nico van Rooijen, Andreas Radbruch, Richard Lucius, Susanne Hartmann, Georg N. Duda, Katharina Schmidt-Bleek

Bone (October 2015)

Fracture healing

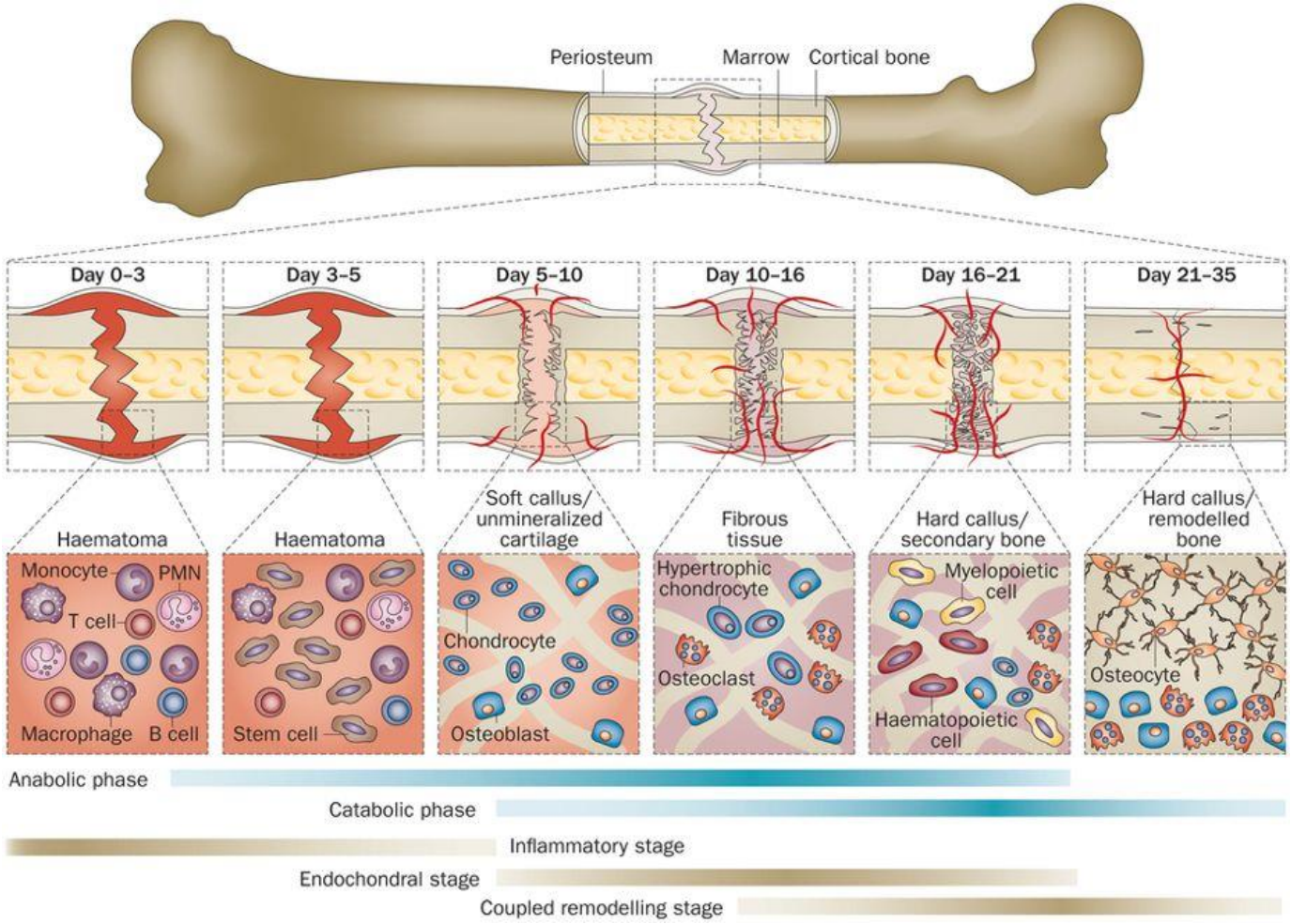

Einhorn et al. (2015)
Nature Reviews Rheumatology

Macrophage subsets

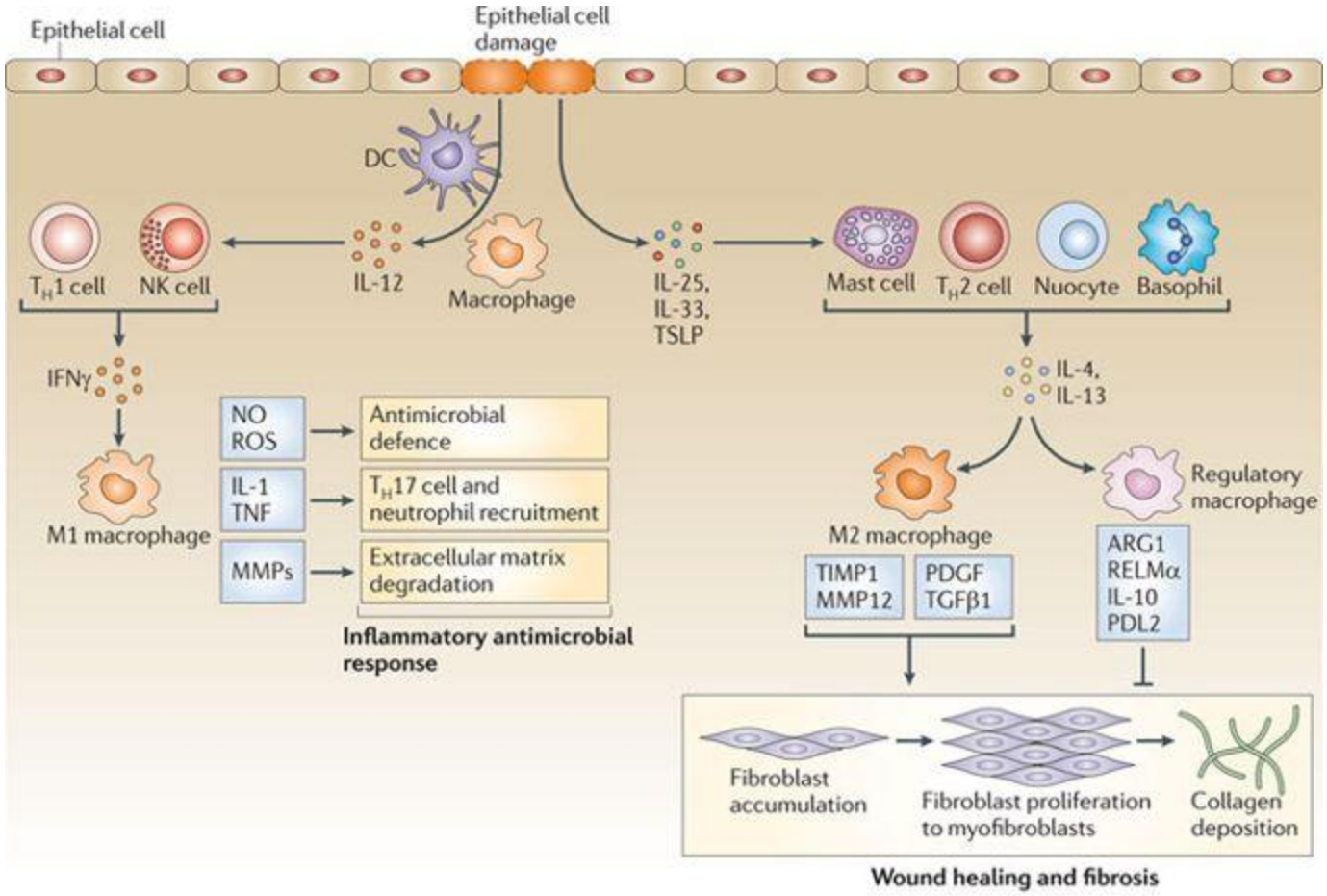

Nature Reviews | Immunology

Murray et al. (2011)

Methods

Animal model and macrophage depletion

Assesment of the role of the macrophages

- 8-week old male mice
- Standardized, unilateral closed fractures were produced in the left femur.
- SPF facility (controlled temperature (20 ± 2 ˚C) with a 12 h light/dark circle and food and water ad libitum)
- Control group (WT)

Macrophage depleted group (MAP): 48h before fracture iv infection of 100 µL clodronate filled liposomes (5 mg/mL) dissolved in 100 µL PBS into the tail vein. → repeated every 5d

Assesment of M1/M2 macrophage phenotype switch

- Female C57BL/6N mice (12 weeks old)
- Lateral-longitudinal incision of the skin (2 mm) along an imaginary line from knee to hip.
- A 0.70 mm osteotomy was performed using a Gigli wire saw. Postoperative analgesia was conducted.
- Animals were euthanized after 1, 3, 7 and 21 days (n= 3).

The inducement of the M2 phenotype

- IL-4 and IL-13 (50 ng) were applied to a collagen scaffold that was inserted into the osteotomy gap upon surgery. A collagen scaffold treated with PBS was inserted in the control group. Bone healing in these animals was analyzed 21 days into healing, n=6.

µCT analysis

- Macrophage depletion: At days 7, 14, 21, and 28 femurs (n=8 each) were scanned with a fixed isotropic voxel size of 10.5 µm. A fixed global threshold of 190 mg HA/cm3 (9 week old male mice) was selected that allowed the rendering of mineralized callus only.
- M2 polarization: At day 21 (n = 6), 240 mg HA/cm3 (12-week-old female mice).

Biomechanical testing

- Fractured and non-fractured femora
- Bones were loaded to failure in torsion at 0.5 °/s with an axial preload of 0.3 N. Ultimate torque and torsional stiffness were measured from torque-rotation curves.

Histological analysis

- Femurs harvested at 3, 7, 14, 21 and 28 days after fracture (Movat-Pentachrome staining).
- The intramembranous areas of the callus at day 14 were analyzed (n = 8) using a computer aided method to determine the areas between the newly formed woven bone in order to determine the porosity.
- Macrophages were stained and investigated using an antibody against CD68. For confirmation of macrophage depleted animals (n=5WT and n= 7 MAC) three independent bone marrow regions were evaluated and positive cells were counted to determine the macrophage numbers.

- Blood vessels were stained with Smooth muscle alpha actin .
- Tartrate resistant acid phosphatase (TRAP) staining for osteoclasts: The cells had to have more than 2 nuclei, show TRAP-positive staining and had to be located on the bone surface.
- Collagen type II and type X: Two steps of antigen retrieval were performed with hyaluronidase and pepsin. Primary antibodies → mouse monoclonal antibodies, secondary antibodies anti-mouseFc IgG
- Further immunofluorescence staining of macrophages: Antibodies → CD68 , CD80 and CD206

µ-Array analysis

- After removal of soft tissue, callus tissue samples were collected. The bone was bisected at a 1 mm distance on either side of the fracture callus (n=5/group per time point). The calli were flash frozen in liquid nitrogen and immediately kept at −80 ˚C until being processed. Samples were first pulverized under continuous cooling with liquid nitrogen then homogenized in TRIzol while kept on ice.

M2 induction in vitro

Whole bone marrow cell isolation:

- From femora and humeri of 12-week-old female C57BL/6 mice (n = 4).
- Mice were kept under semi-sterile conditions (for immune system activation) for at least 4 weeks prior to the experiment.
- After flushing the bone marrow cells from the bone with sterile syringes and RPMI 1640 containing 2 mM L-glutamine, bone marrow cells were cultured at a concentration of 2. 5× 10^6/mL in this RPMI, supplemented with 10% fetal bovine serum, 1% penicillin and streptomycin, and 50 µM b-mercaptoethanol.

M2 induction in vitro

Macrophage polarization:

- Monocytes and macrophages contained in whole bone marrow cells were polarized to M2 macrophages for 48 h at 37 ˚C with IL-4 and IL-13 (recombinant human cytokines IL-4, IL-13) applied at final concentrations of 20 ng/mL or left untreated as control.
- The untreated control culture contained PBS with the same volume of the applied interleukins. After 48 h cells were harvested and investigated via flow cytometry.
- Cells were transferred to 100 µL FACS buffer (500 mL PBS, 1% BSA, 0.1% Na3N) and staining was performed for 20 min in the dark on ice: CD68 , CD80 , CD86, CD206, CD163, and LIVE/ DEAD stain kit. Cells were fixated in 2% formalin/PBS.

Results

Macrophage depletion

- A 65% macrophage reduction was achieved by the clodronate liposome treatment.
- Osteoclast numbers in the fracture callus were not significantly altered.

Macrophage depletion results in a delayed healing

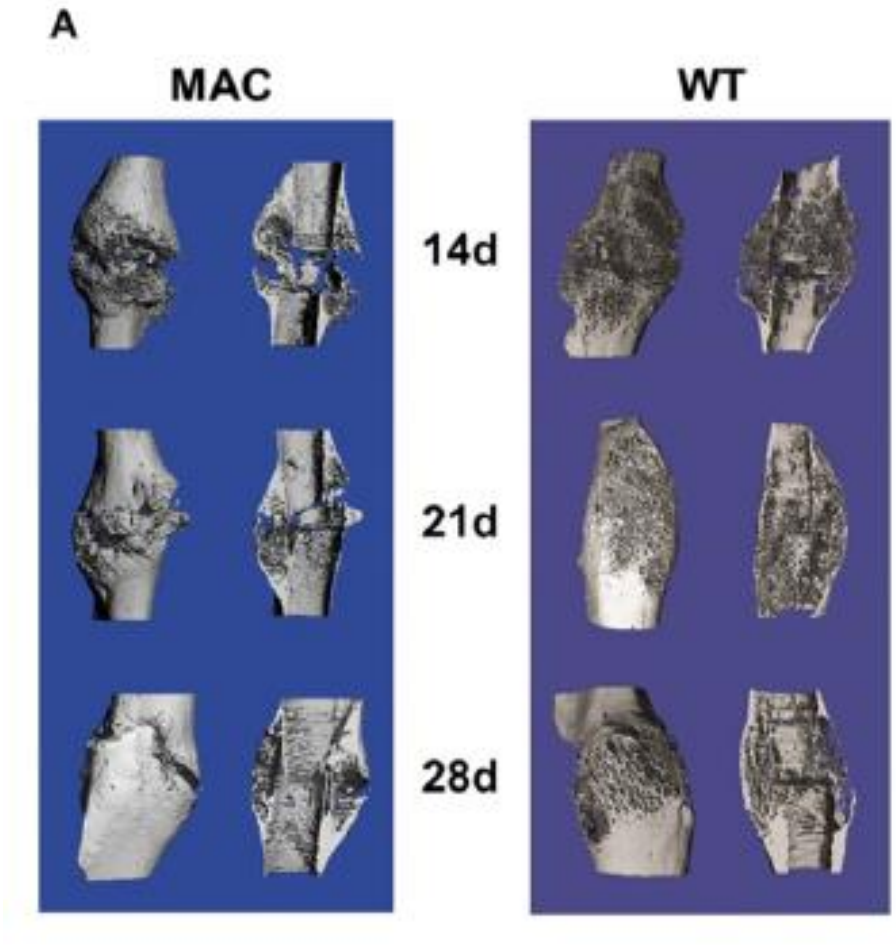

Fig. 1. Representative 3D image reconstructions (entire callus, longitudinal section) of WT vs. MAC fracture calli at days 14, 21 and 28 after fracture.

Macrophage depletion results in a delayed healing

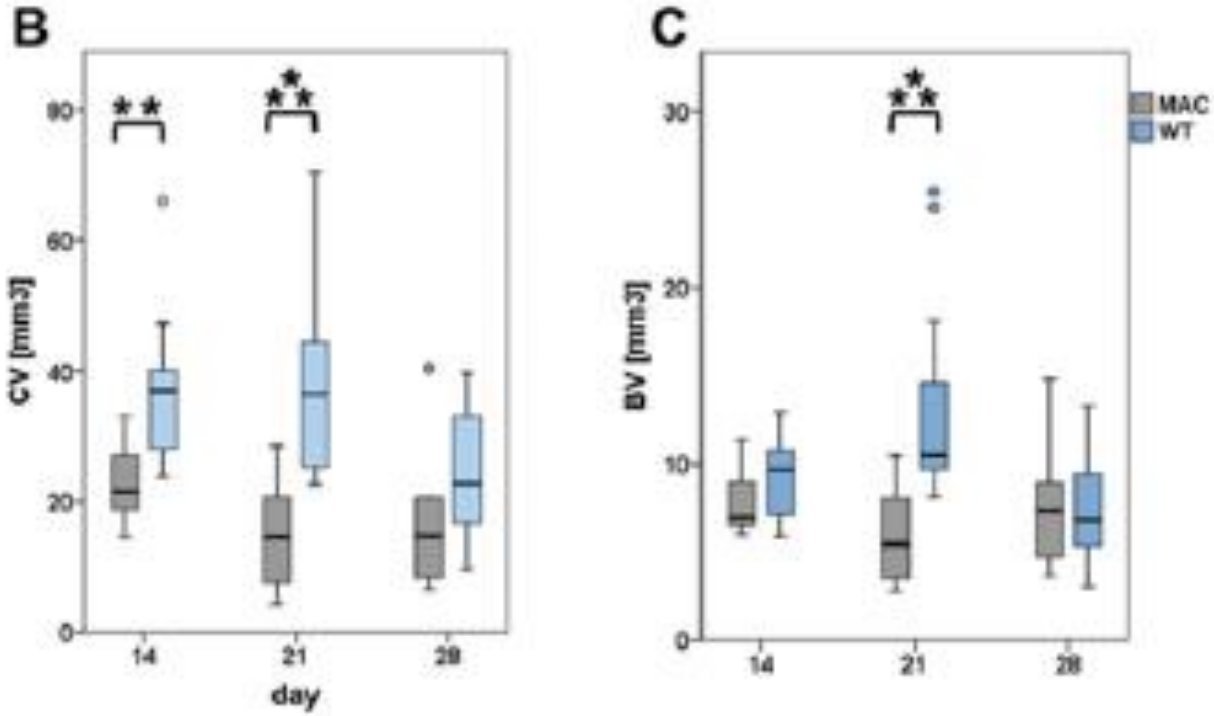

Fig. 1 Callus and bone volume

Macrophage depletion results in a delayed healing

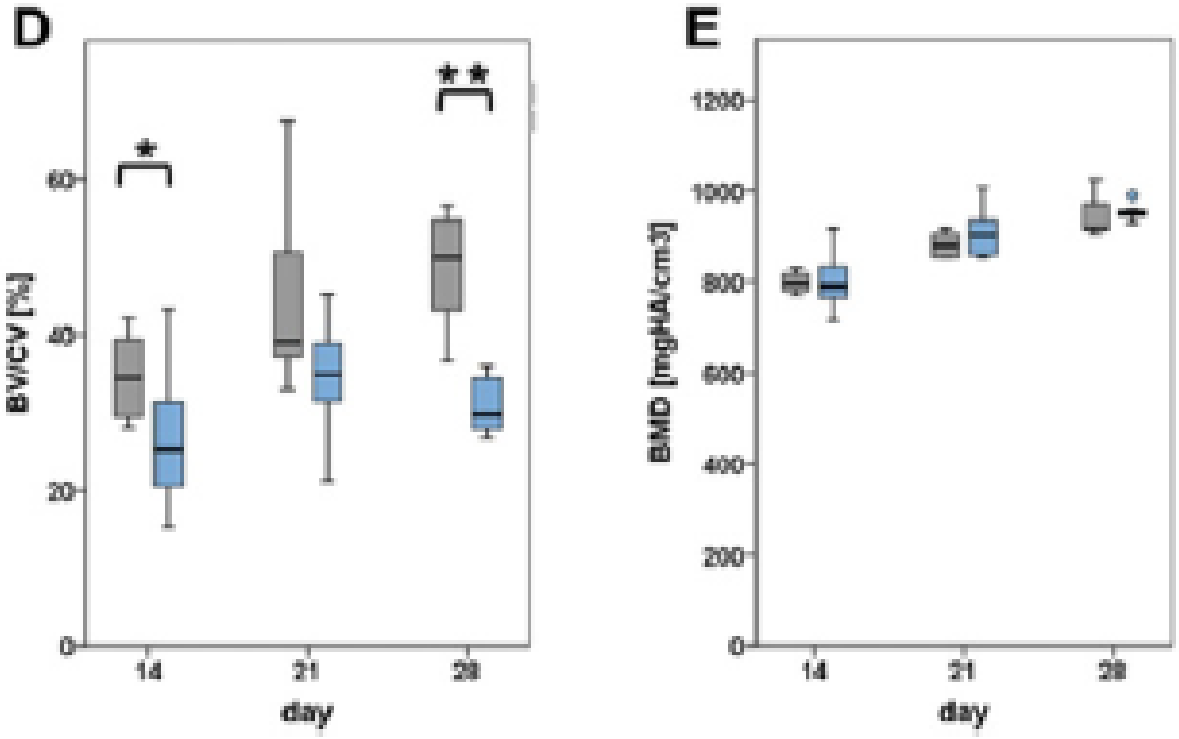

Fig. 1 BV/CV percentage and bone mineral density

Macrophage depletion results in a delayed healing

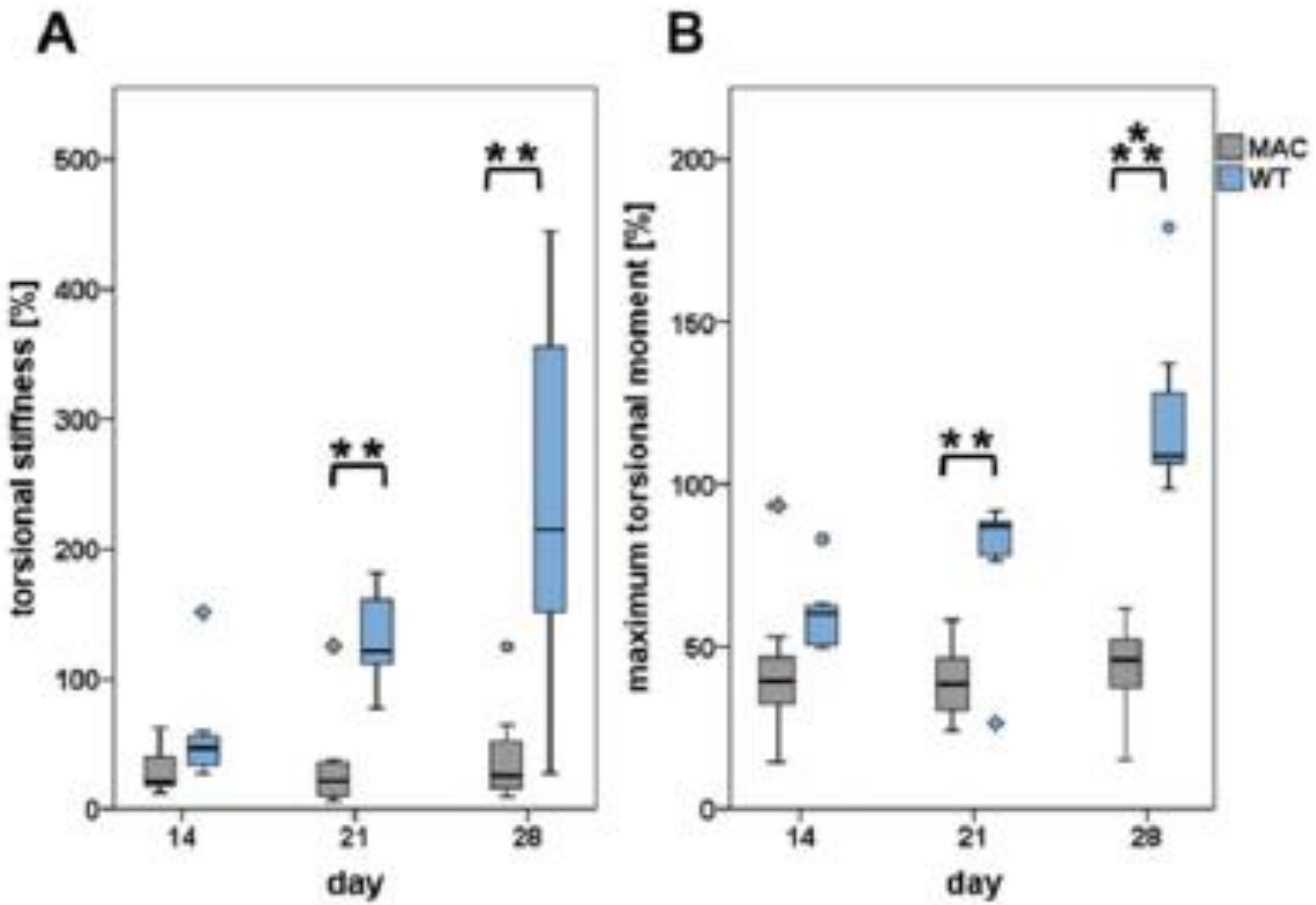

Fig. 2. Graphic presentation of quantitative data of biomechanical testing of fractured bone. Biomechanical properties of healing fractures were severely altered in the MAC group. Maximum torsional moment and torsional stiffness were significantly lower in animals healing with a reduced macrophage number at day 21 and 28 after fracture. Values are reported in relation to unfractured contralateral bones. The results of a student t-test are given on each plot: **p b 0.01, ***p b 0.001, n = 8 each.

Delayed cartilage resorption cause of disturbed endochondral ossification

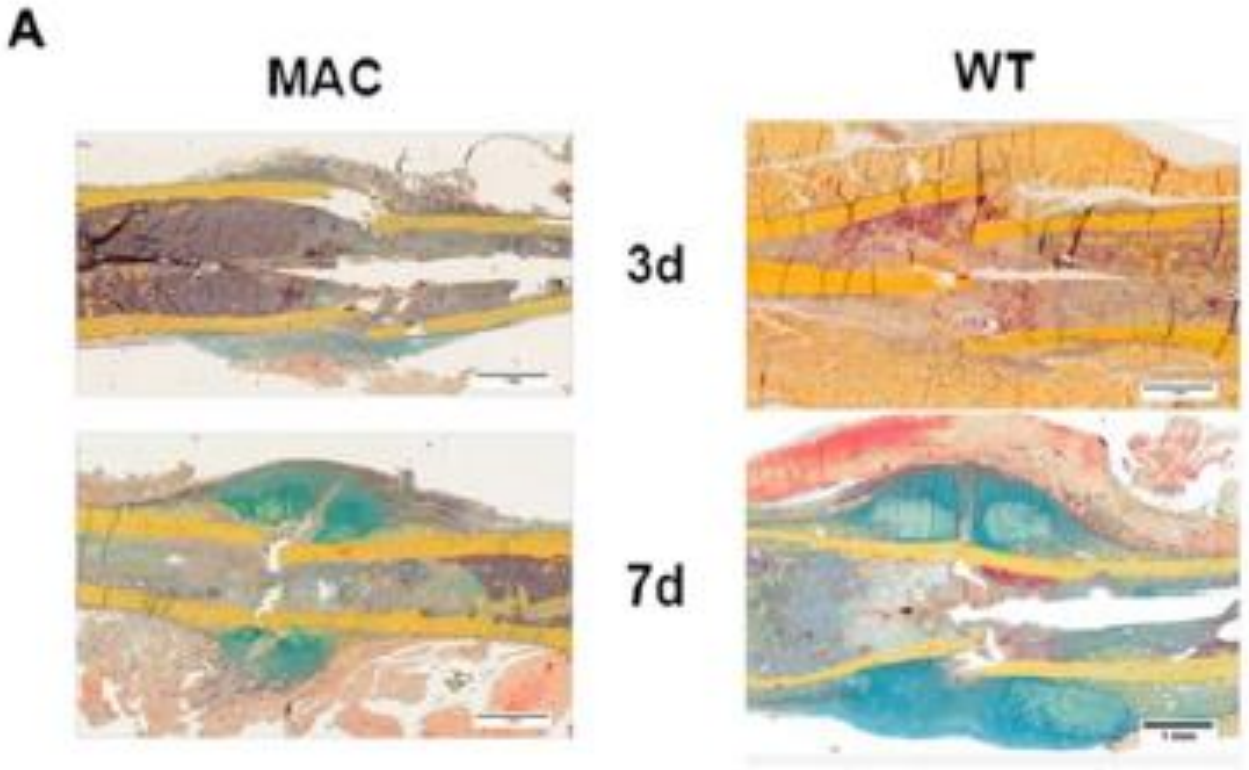

- **Fig. 3**. Histological sections of WT vs.MAC fractures at days 3, 7, 14, 21 and 28 after fracture, Movat pentachrome staining: mineralized tissue — yellow; cartilage — blue/green; muscle — red; bone marrow— purple. The WT showed physiological healing with completed endochondral ossification at day 21. Here, bony bridging was accomplished through a trabecular callus filled with bone marrow. In contrast, the MAC showed delayed healing. The MAC callus was small and immature, cartilage resorption and endochondral bone formation were not completed until day 28 (n = 8 each).

Delayed cartilage resorption cause of disturbed endochondral ossification

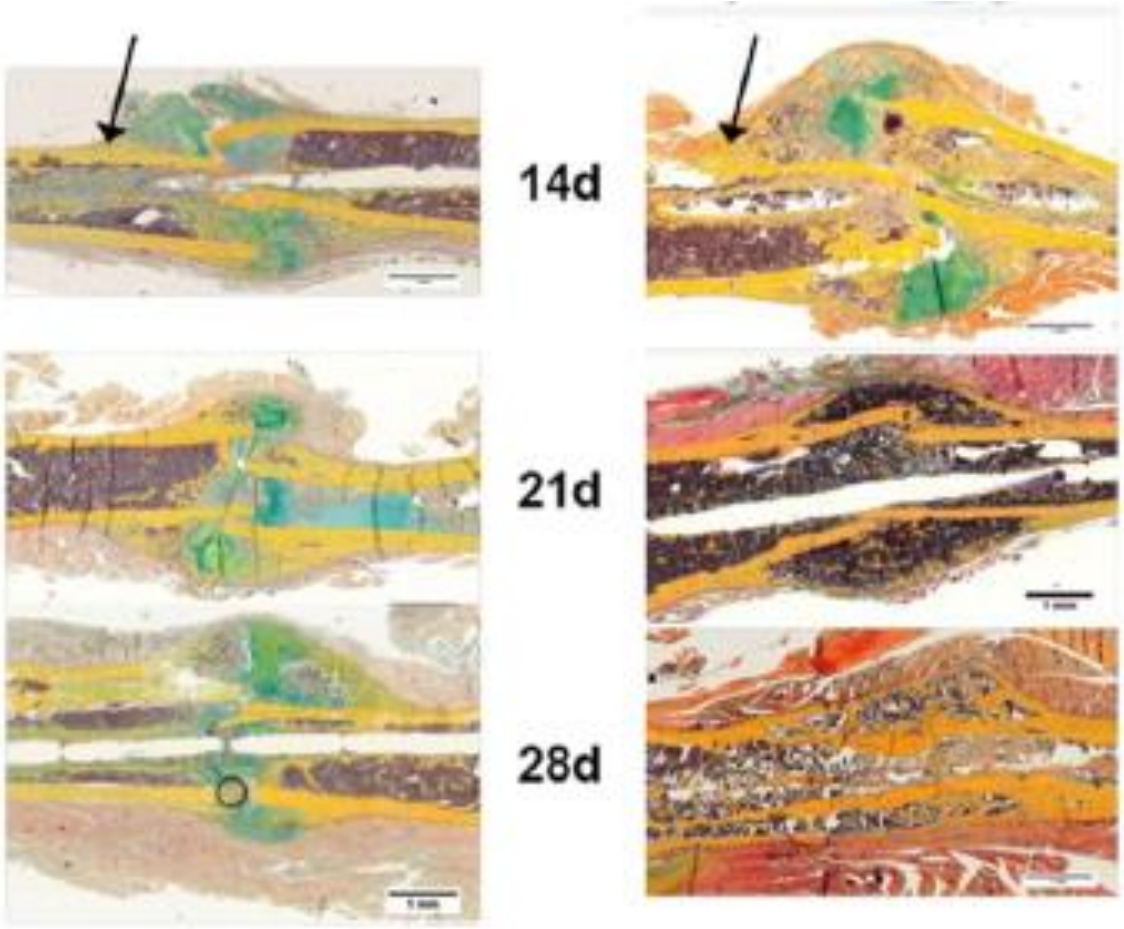

Fig. 3. Histological sections of WT vs.MAC fractures at days 3, 7, 14, 21 and 28 after fracture, Movat pentachrome staining: mineralized tissue — yellow; cartilage — blue/green; muscle — red; bone marrow—purple. The WT showed physiological healing with completed endochondral ossification at day 21. Here, bony bridging was accomplished through a trabecular callus filled with bone marrow. In contrast, the MAC showed delayed healing. The MAC callus was small and immature, cartilage resorption and endochondral bone formation were not completed until day 28 (n = 8 each). Arrows indicate exemplary areas of intramembranous ossification.

Delayed cartilage resorption cause of disturbed endochondral ossification

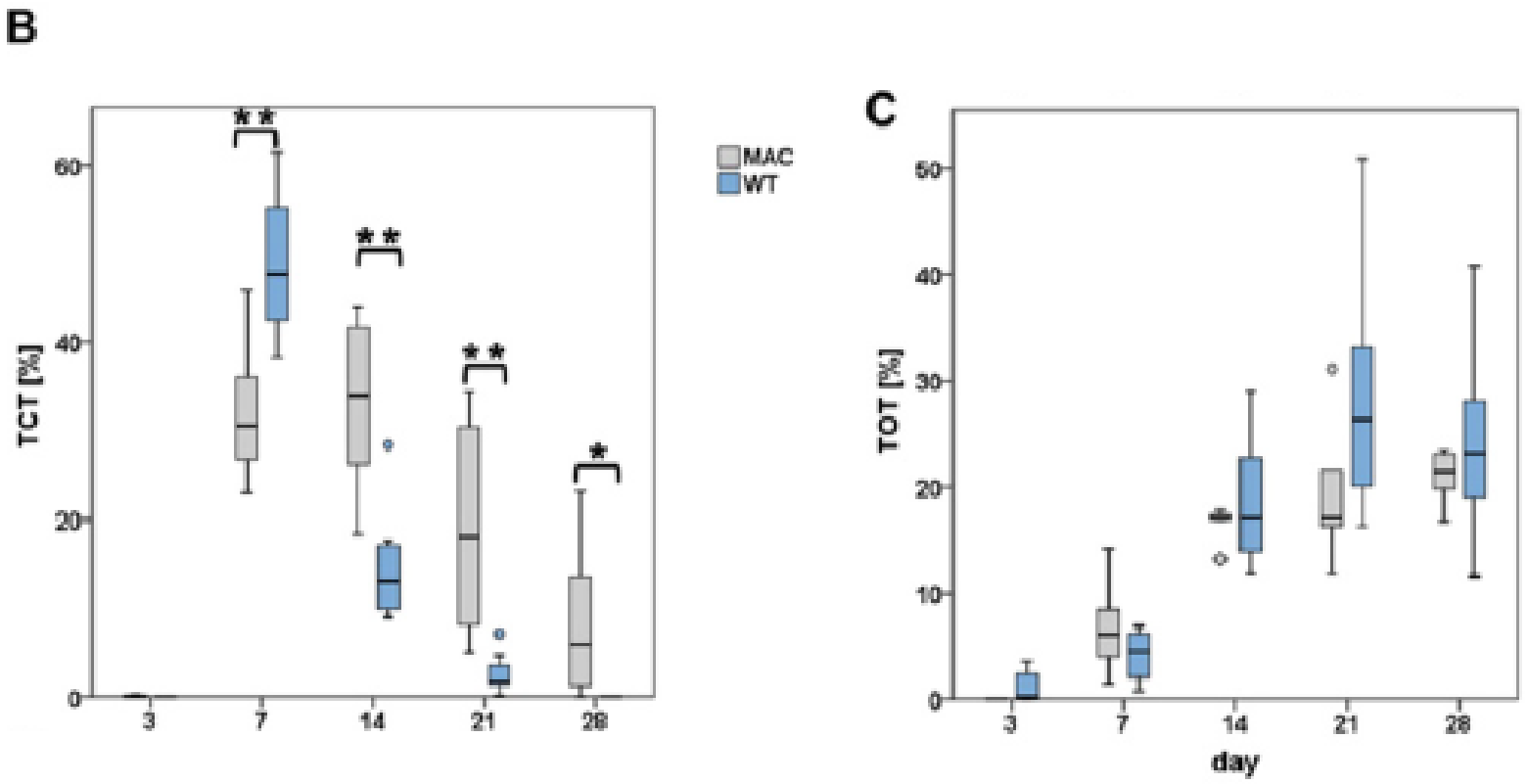

Fig. 3. Histomorphometrical analysis showed a fast increase of cartilage (7 days) in the WT with a consecutive reduction and final resolution around day 28 (TCT — total cartilage tissue). In the MAC animals cartilage remained significantly elevated from day 14 until 28 in comparison with the normal healing pattern. Total osseous tissue (TOT) on the other hand did not show significant differences between the two groups over the course of healing. The results of a student t-test are given on each plot: *p b 0.05, **p b 0. 01, n = 8 each).

Delayed cartilage resorption cause of disturbed endochondral ossification

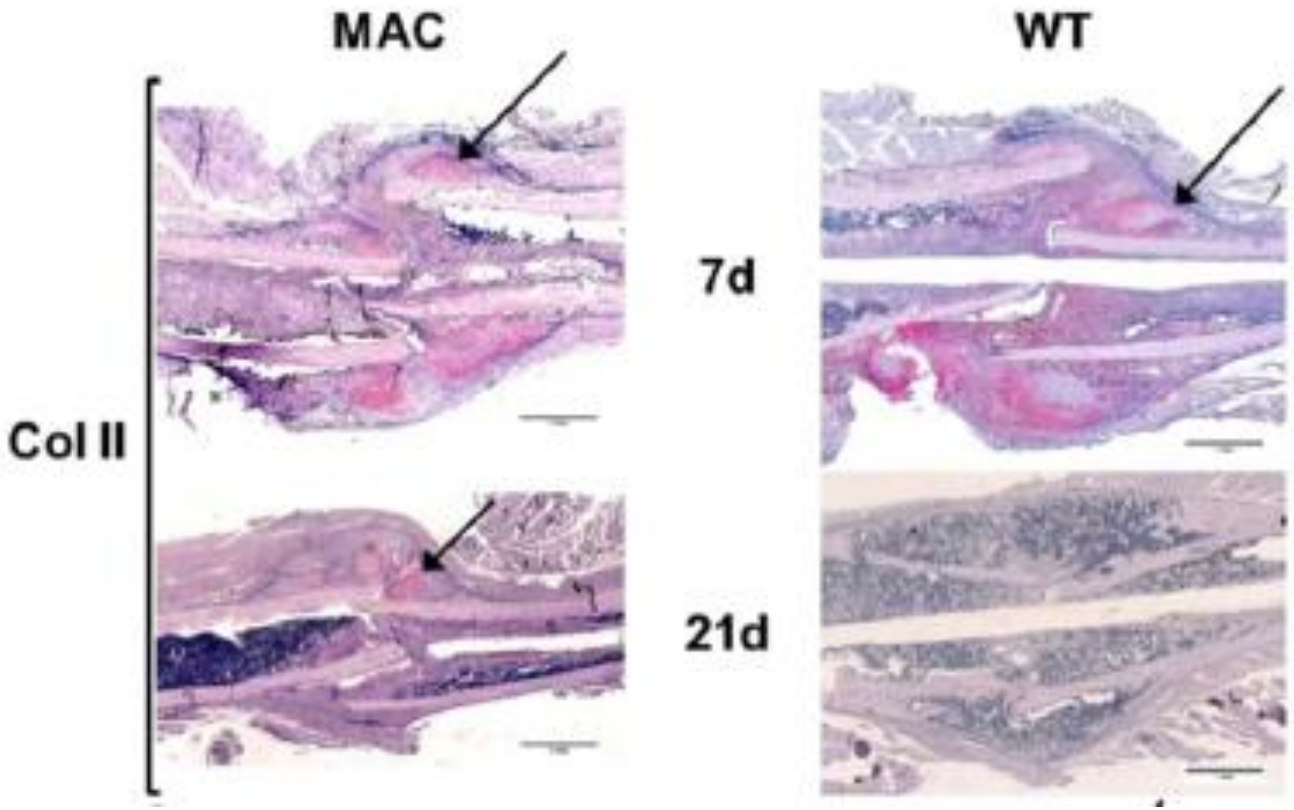

Fig. 4. Immunohistochemistry of fracture callus for cartilage specific collagens II and X at days 7 and 21. At day 7, Col II and Col X can be detected in WT and MAC animals, as indicated by the arrows. At day 21 both collagens are absent in WT animals but still being observed in MAC fracture callus (highlighted by the arrows). This is an indication that endochondral bone formation is impaired in the absence of macrophages. Scale bar = 1 mm.

Delayed cartilage resorption cause of disturbed endochondral ossification

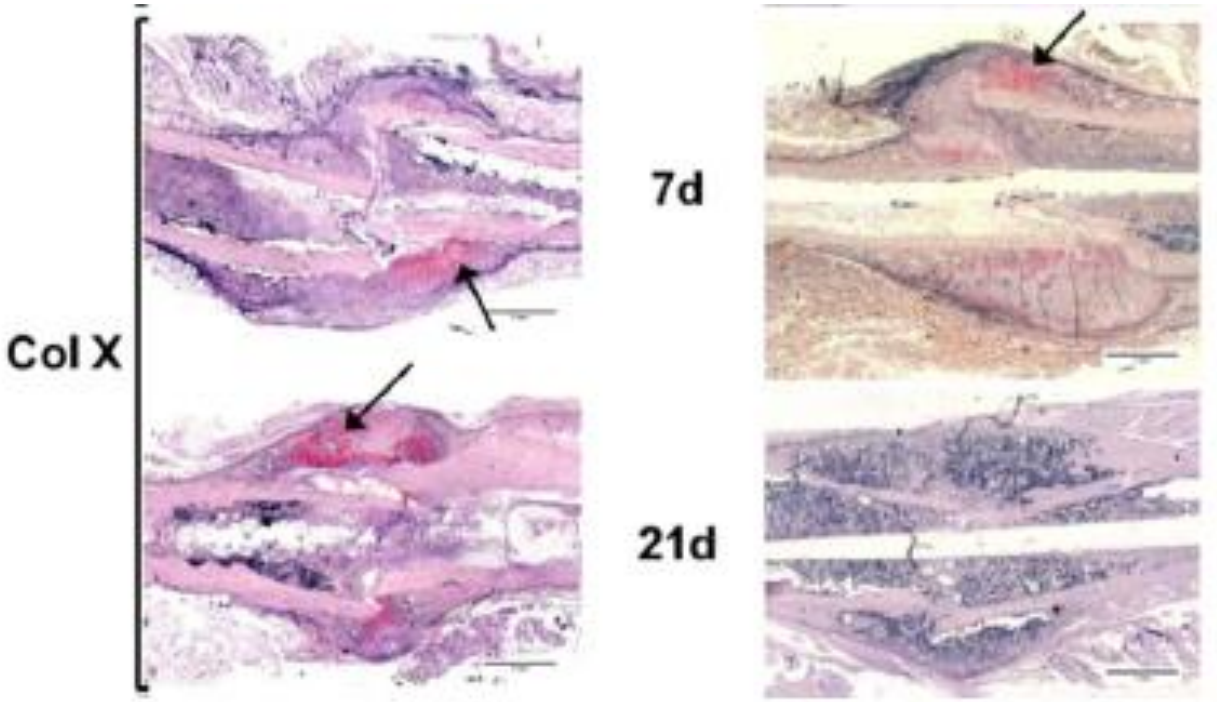

Fig. 4. Immunohistochemistry of fracture callus for cartilage specific collagens II and X at days 7 and 21. At day 7, Col II and Col X can be detected in WT and MAC animals, as indicated by the arrows. At day 21 both collagens are absent in WT animals but still being observed in MAC fracture callus (highlighted by the arrows). This is an indication that endochondral bone formation is impaired in the absence of macrophages. Scale bar = 1 mm.

Macrophages impact intramembranous ossification

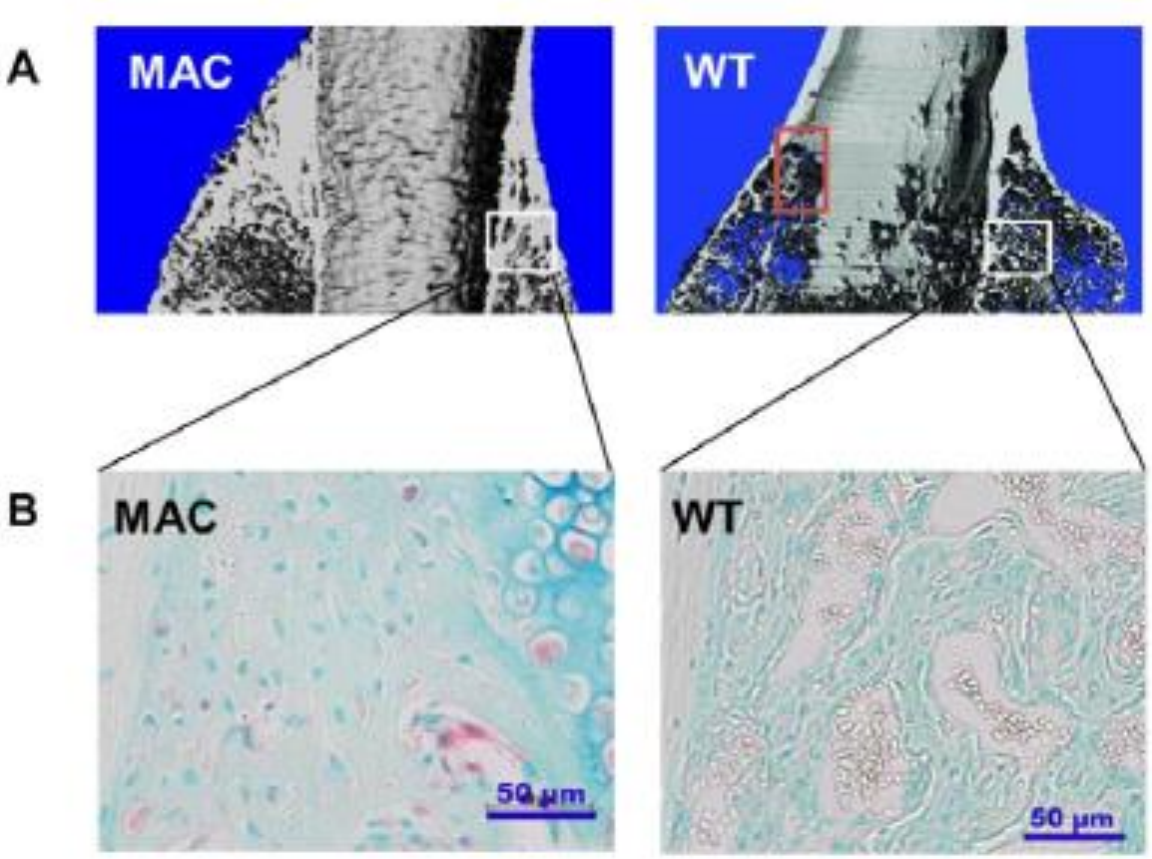

Fig. 5. µCT images of the periosteal ossification 14 days after fracture (A) clearly show the difference in tissue organization with a denser mineralization area in the MAC group. The areas where intramembranous ossification takes place (highlighted by gray rectangles) clearly show smaller erythrocyte filled spaces in the MAC group, probably due to a reduced ECM remodeling after macrophage depletion (B).

Macrophages impact intramembranous ossification

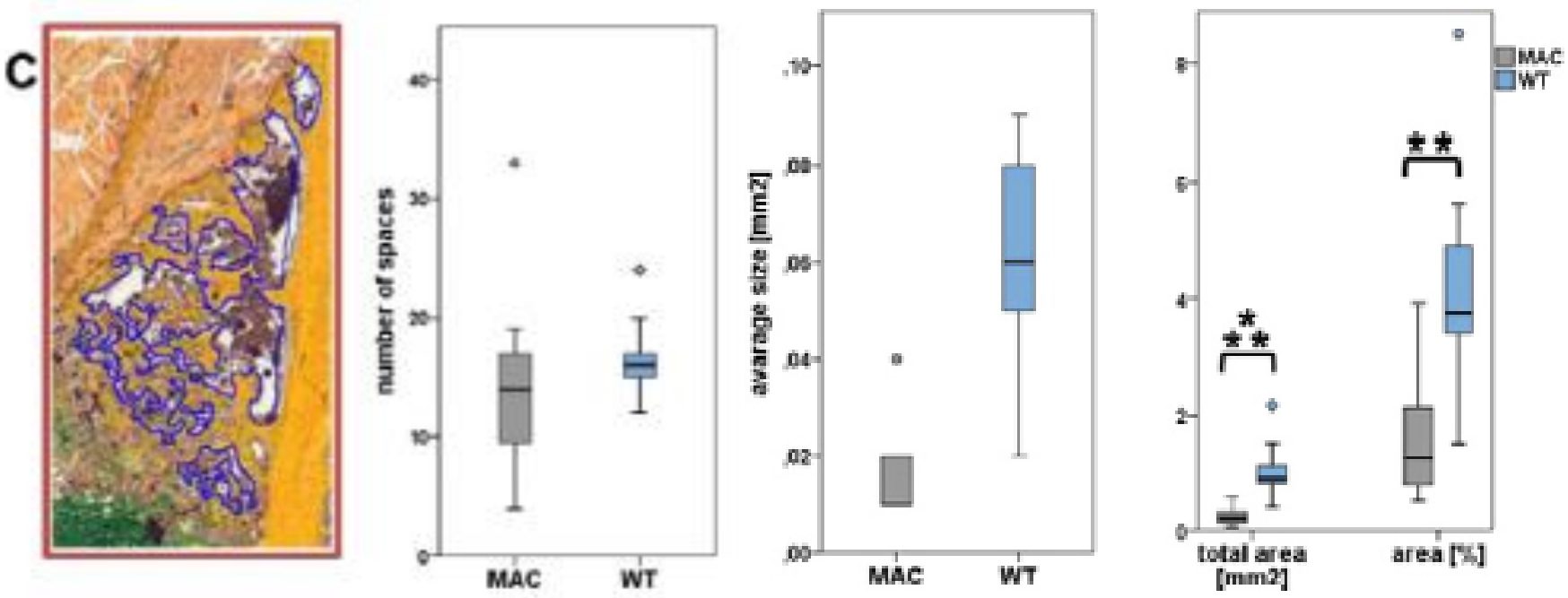

Fig. 5. (C) Spaces between the woven bone trabeculae have been measured (region is indicated by red rectangle). While the overall number of spaces is only slightly lower in the MAC animals, the average size of the spaces is reduced. This leads to a significantly smaller bone free area in the periosteal callus region both in total (***p = 0.001) and in percentage (**p = 0.004).

Gene expression changes in macrophage and ossification related genes corroborate results

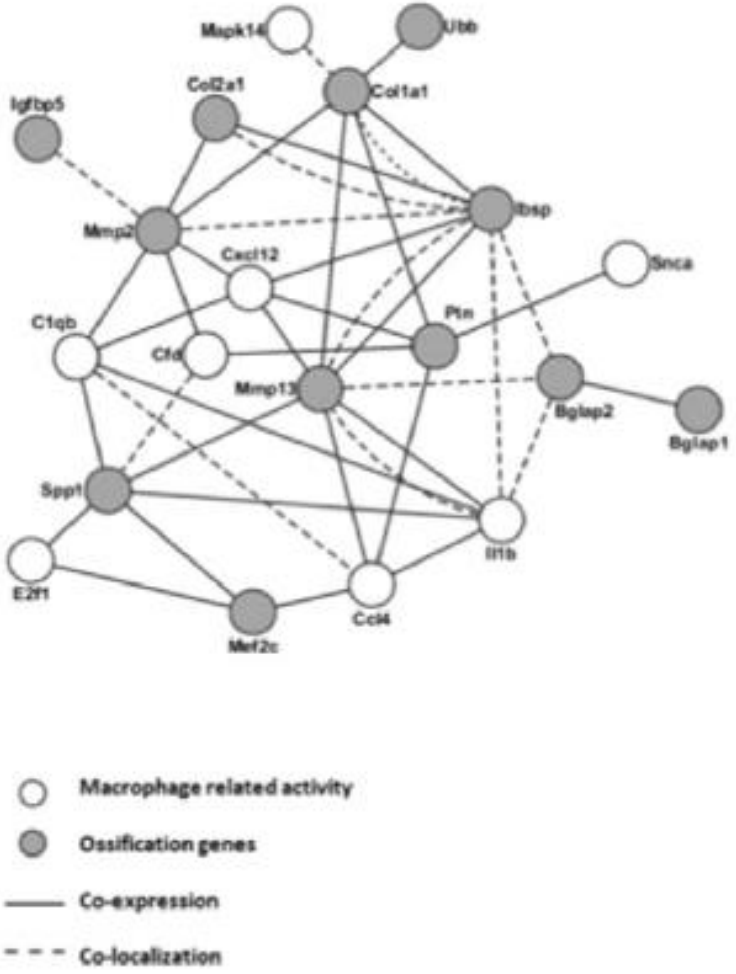

Fig. 6. In the network created by "guilt of association" the interconnecting genes are depicted.

Gene expression changes in macrophage and ossification related genes corroborate results

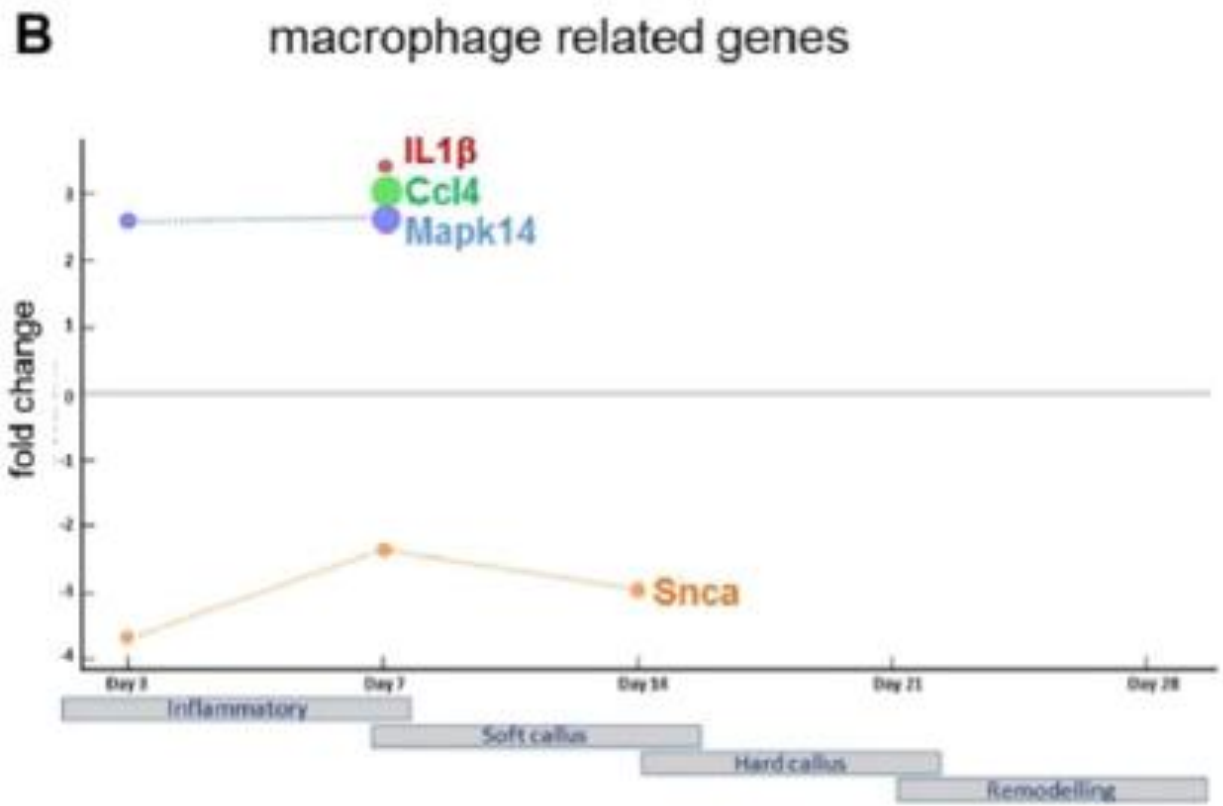

Fig. 6. Regulation of ossification and macrophage related change throughout bone healing in MAC mice compared to WT mice. Negative fold change indicates down-regulated genes; positive fold change indicates up-regulated genes.

Gene expression changes in macrophage and ossification related genes corroborate results

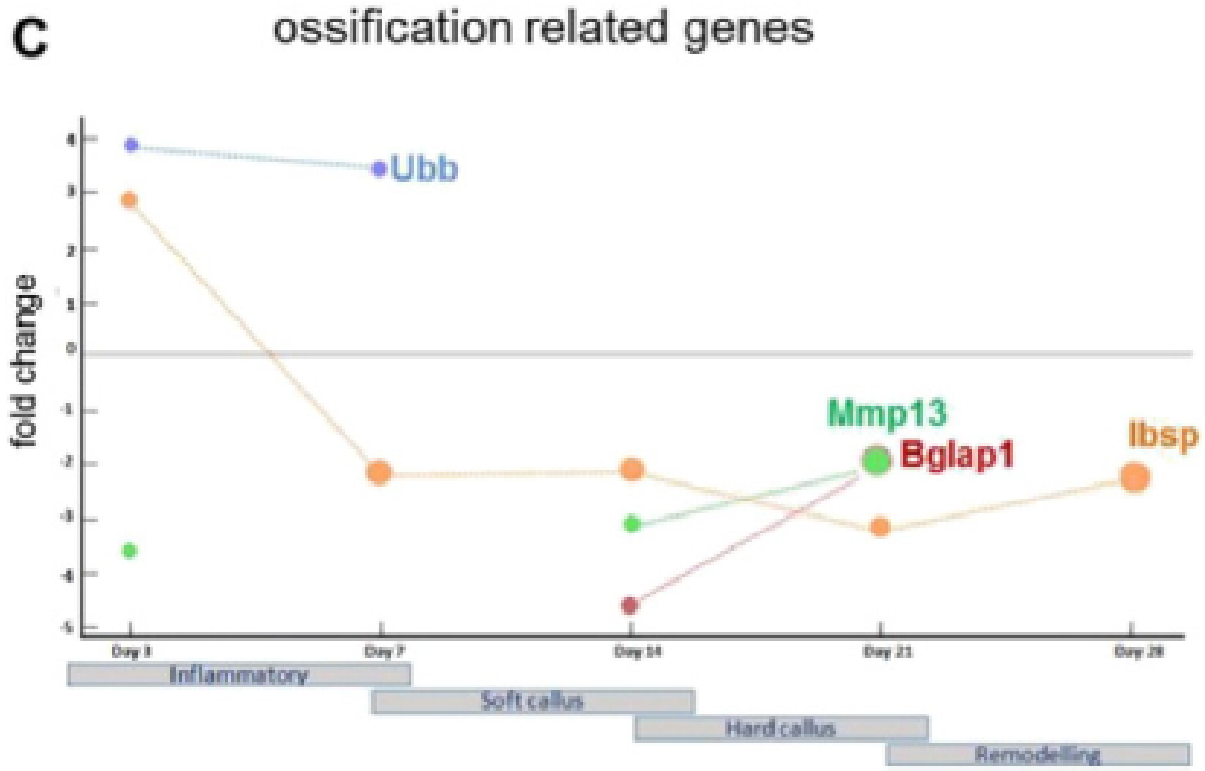

Fig. 6. Regulation of ossification and macrophage related change throughout bone healing in MAC mice compared to WT mice. Negative fold change indicates down-regulated genes; positive fold change indicates up-regulated genes.

Macrophages change their phenotype during the course of bone healing

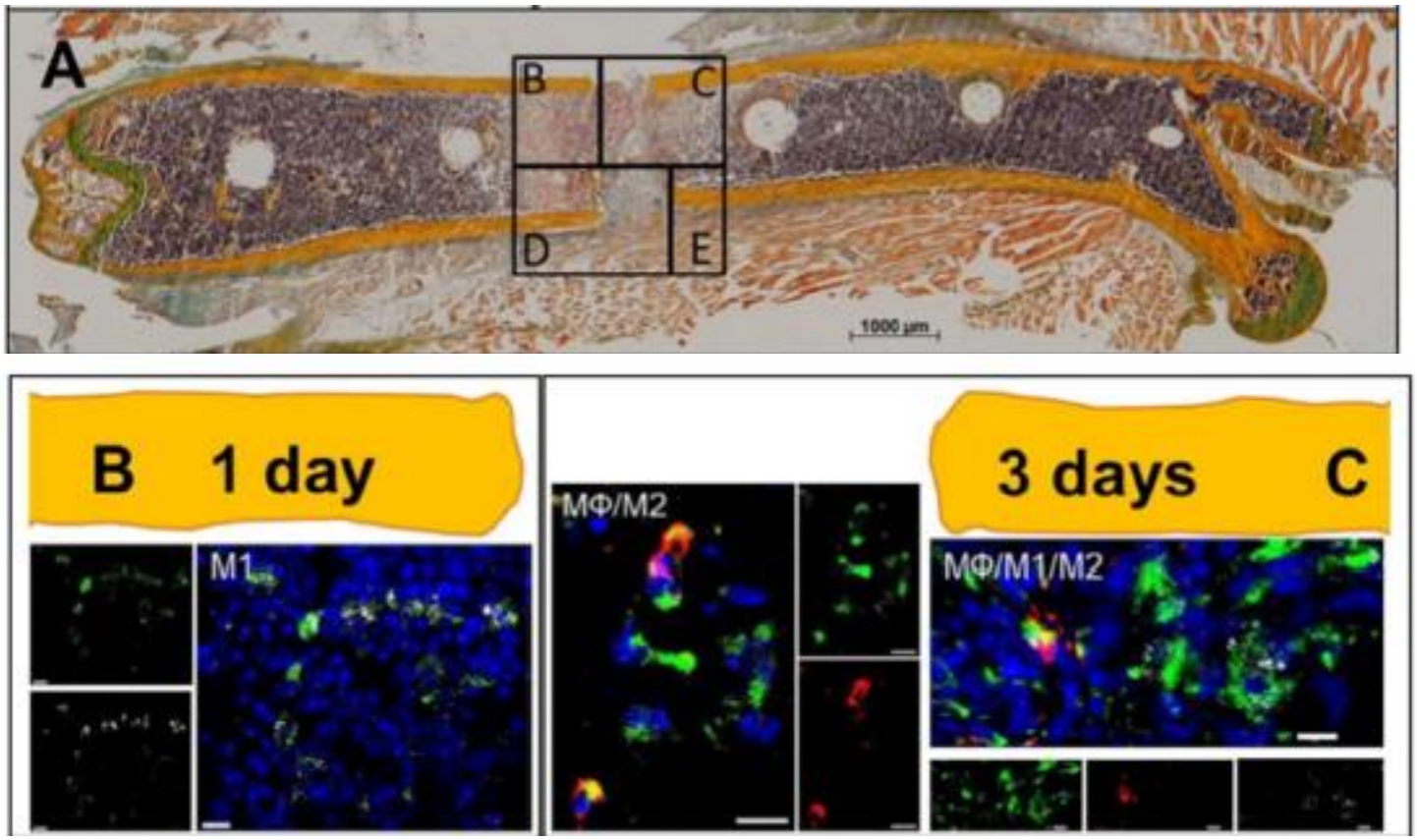

Fig. 7. M1 and M2 macrophages are present during different stages of fracture healing in a mouse osteotomy model. Movat pentachrome staining of a wild type murine femur 7 days post osteotomy (A), the complete rectangle presents the osteotomy area in which the existence of macrophages of different polarization states was analyzed and the four smaller rectangles schematically depict areas of the pictures B-E; predominantly pro inflammatory1macrophages are found in the osteotomy area 24 h post-osteotomy(B); after 3 days post-surgery, antiinflammatory M2 macrophages infiltrate the osteotomy area from the muscles (C).

Macrophages change their phenotype during the course of bone healing

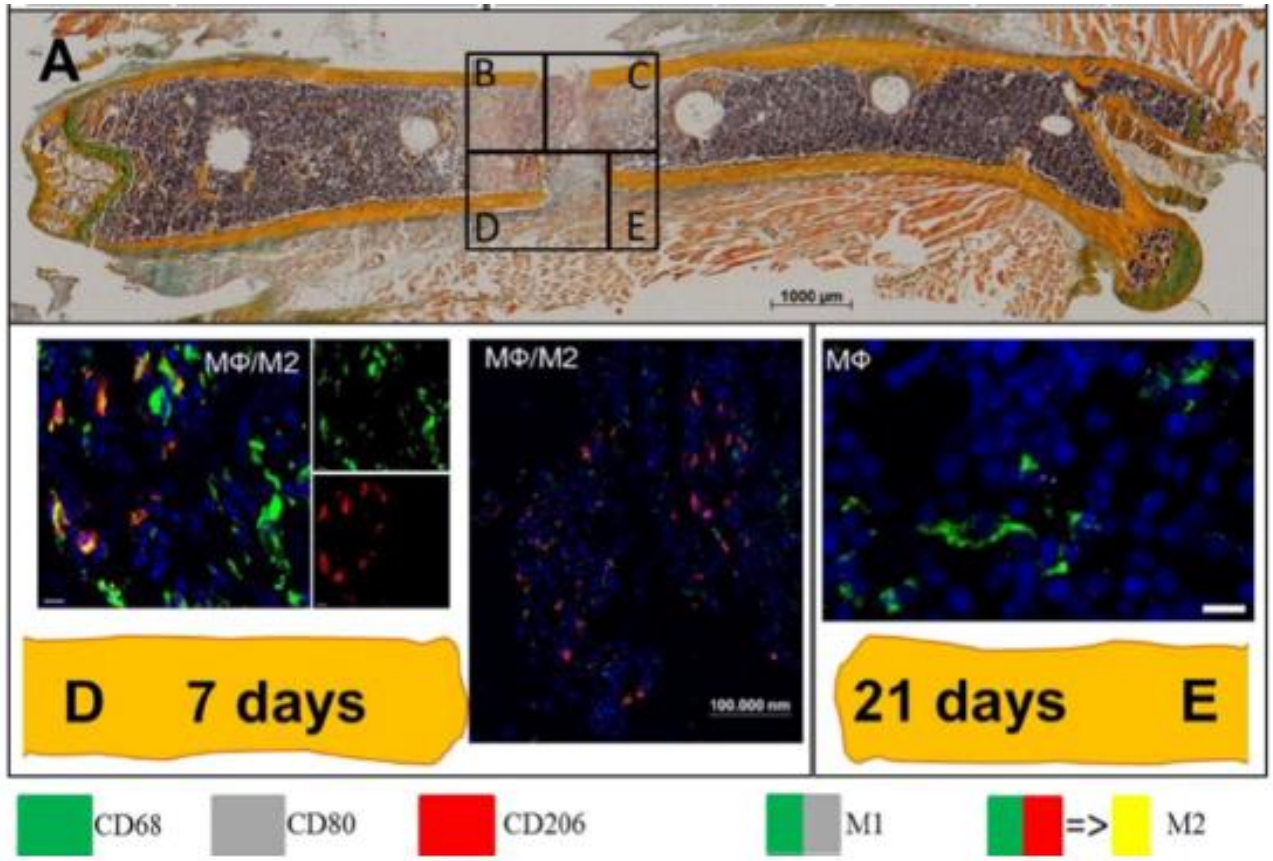

Fig. 7. Predominance of M2 macrophages 7 days after setting the osteotomy (D); 21 days post-osteotomy, almost only MΦ macrophages are present in the former osteotomy area (E); blue = DAPI, green = CD68 (MΦ), gray = CD80 (M1), red = CD206 (M2); scale bar = 10 µm (besides otherwise indicated).

Enhancing M2 macrophages in vivo improves bone regeneration

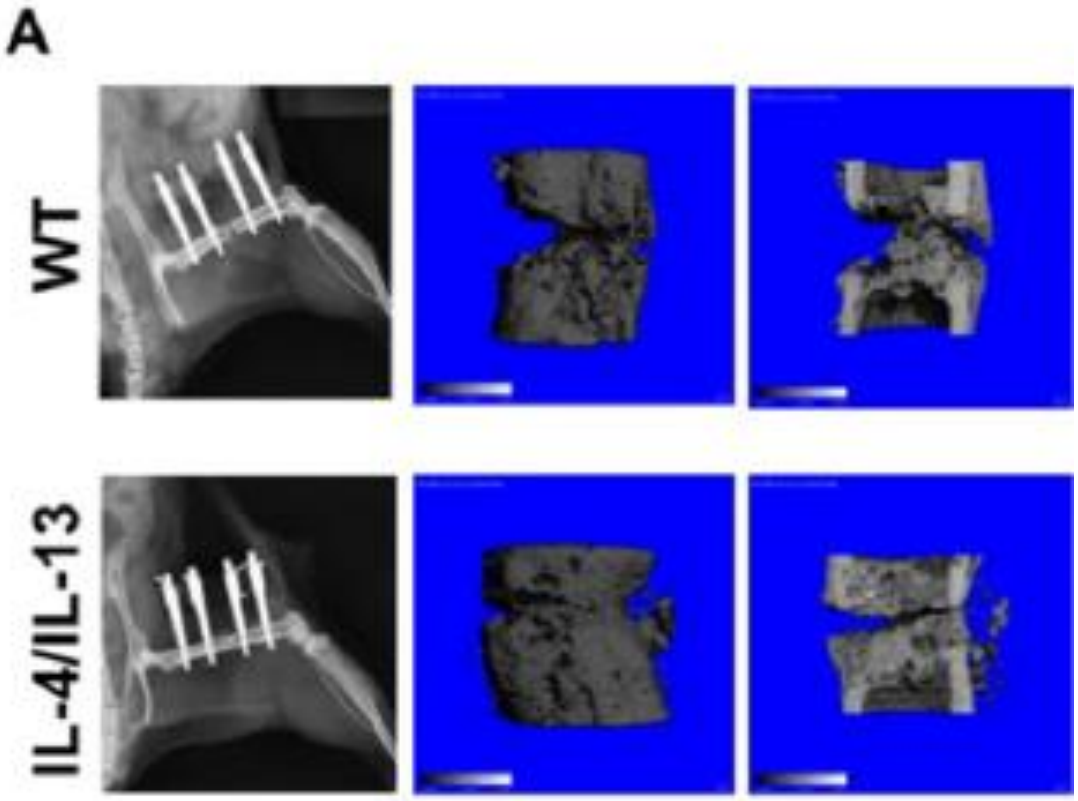

Fig. 8. Comparison of the bone healing outcome after 21 days of healing with M2 phenotype induction via IL4/IL13. An external fixation osteotomy mouse bone healing model was analyzed by µCT, 3D images of both groups (WT and IL-4/IL-13) are shown (A).

Enhancing M2 macrophages in vivo improves bone regeneration

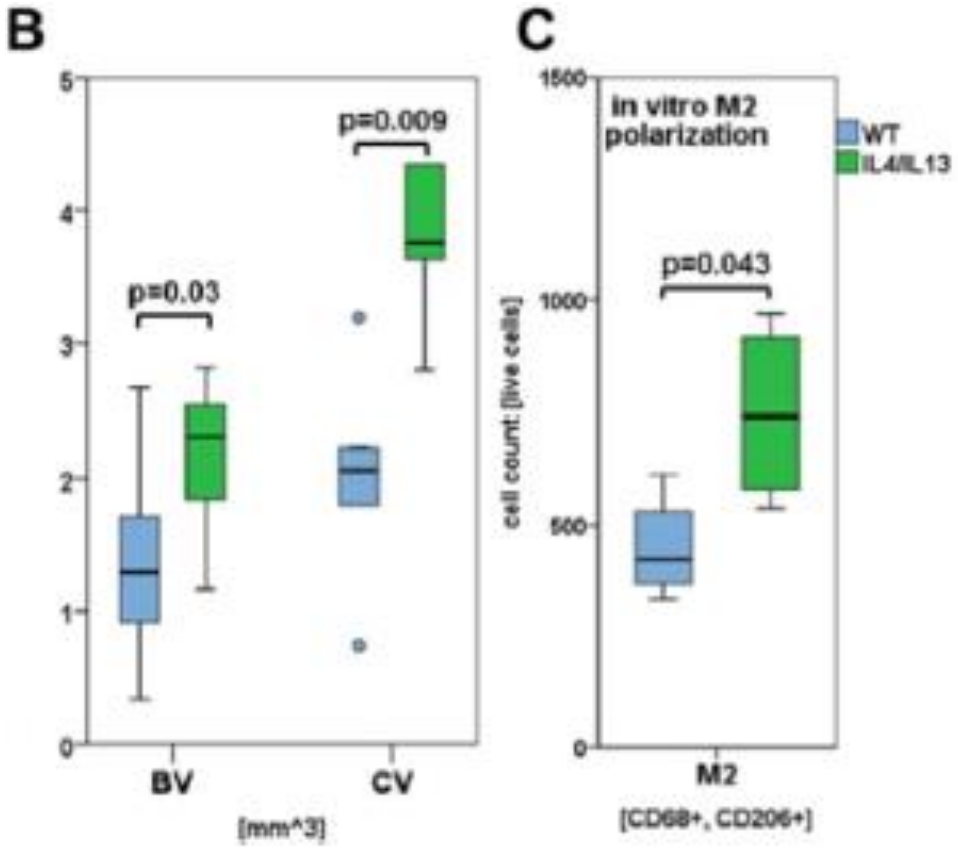

Fig. 8. Total callus volume (CV) as well as the bone volume of this callus (BV) were significantly increased in comparison to the wild type group after induction of M2 macrophages via IL4 and IL13 in the initial phase of healing (Mann Whitney U; n = 5–6) (B). Polarization of M2 macrophage phenotype was confirmed in vitro with freshly isolated murine bone marrow cells: after addition of IL-4/IL-13 the percentage of M2 macrophages (CD68+, CD206+) significantly increased (t-test; n= 4) (C).

Discussion

- Whether macrophages influence the healing phase directly (i.e. Macrophages themselves perform the transformation) or indirectly has to be further analyzed.
- Although the results highlight the tremendous alterations in bone regeneration due to a decreased macrophage population, it is not clear whether these alterations are a consequence of a disturbed early (pro-/anti-inflammatory) phase or a result of both, a disturbed early healing stage and an impairment of chondrogenic callus remodeling at later occurring regenerative processes.

Conclusion

- An impaired macrophage function severely delays endochondral ossification.
- Shifting the inflammatory reaction towards M2 upon treatment of aged individuals could improve the healing outcome and more importantly could help to faster mobilize patients after injury by preventing delayed bone regeneration.

Thank you for listening!